



# Preparation of UV-curable waterborne poly(thiourethane-urethane) acrylate based on thiol-click chemistry

Yali Xiang, Juan Du , Yan Luo

Received: 12 August 2022 / Revised: 22 November 2022 / Accepted: 27 November 2022  
© American Coatings Association 2023

**Abstract** New strategies for synthesizing click chemical reactions have been studied and widely used in the synthesis of functional polymers. In this paper, based on thiol-click chemistry, thiocarbamate bonds and thioether bonds were introduced into the polymer skeleton, and then pentaerythritol tetraacrylate (PETTA) was introduced into the system to form an interpenetrating network structure (IPN). A new type of waterborne poly(thiourethane-urethane) acrylate (WPTUA) coating with strong toughness, high hardness, and rapid curing was obtained. Under the condition of an organotin catalyst, a WPTUA composite dispersion was prepared by using isophorone diisocyanate and polycarbonate diol as monomers, 2-dimethylol propionic acid as a hydrophilic chain extender, trimethylolpropane tris(3-mercaptopropionate) (TMPMP) and PETTA. The molecular structures of intermediate waterborne poly(thiourethane-urethane) (WPTU), WPTUA oligomers and UV-cured polymers were investigated by FTIR spectroscopy and Raman spectroscopy. The effects of the content of TMPMP and PETTA on the properties of WPTUA, including dispersion stability, thermal properties, mechanical properties, water resistance, hardness, and toughness, were investigated. It is found that when the WPTUA dispersion has 16 wt% TMPMP and 28 wt% PETTA, the prepared films have high hardness, significant water resistance and good thermal stability for coating applications on delicate substrates, such as paper, plastic and wood.

**Keywords** Waterborne polyurethane, UV-curable coatings, Thiol-click chemistry, Coating

## Introduction

UV-curable coatings are green and environmentally friendly coatings. However, the current UV-curable polyurethane dispersion coatings have some main defects, such as uneven crosslinking, high brittleness and oxygen inhibition.<sup>1,2</sup>

Thiol-click chemistry has been extensively used in the synthesis of polymers due to the ease of S–H bonding for anionic or radical-mediated polymerization reactions, which takes advantage of rapid reactions and can exhibit a homogeneous crosslinked network structure under mild conditions.<sup>3–5</sup> Emerging synthetic strategies for thiol-ene, thiol-alkyne<sup>6</sup> and thiol-isocyanate<sup>7</sup> click reaction concepts can be used to design reactive polymers for environmentally friendly polyurethane coatings. Among them, the thiol-isocyanate click reaction offers a facilitated synthesis method for functional thiopolyurethane. The resulting hydrogen bond can show a higher extent of mixing of soft and hard segments and improve the properties of materials.<sup>8</sup> The thioether bond obtained from the thiol-ene reaction is used in UV-curable waterborne coatings to prevent oxygen blocking polymerization.<sup>9</sup>

Yang<sup>10</sup> et al. prepared a coating containing a mixture of polyfunctional mercaptan and polyfunctional alkene terminated PU aqueous dispersions. By combining thiol-ene click chemistry, the polymerization speed of the coating under air conditions was increased by 1.5 times with the effect of antioxidant blocking, and Young's modulus and tensile strength at the break of the film were increased by 25% and 10%, respectively. Chen<sup>11</sup> et al. functionalized the efficient side chain of castor oil by a thiol-ene photochemical method for the first time and then reacted it with isocyanate polyur-

Y. Xiang, J. Du (✉)  
College of Chemistry, Chemical Engineering &  
Biotechnology, Donghua University, Shanghai 201620,  
China  
e-mail: dujuan@dhu.edu.cn

J. Du, Y. Luo  
Key Laboratory of Science & Technology of Eco-Textile,  
Ministry of Education, Donghua University, Shanghai  
201620, China

ethane to synthesize UV-curable castor oil-based multifunctional polyurethane acrylate.  $^1\text{H}$  NMR analysis showed that the C=C groups were cured completely within 10 min. In addition, the resin exhibited a good UV-curable rate. Based on click chemistry, Konuray<sup>4</sup> et al. prepared novel allyl functional catalytic copolymer monomers. The monomer is combined with thiol by a thiol-ene reaction to the polymer network. The final material obtained by the modified reaction is clear, transparent and presents a uniform network structure.

However, there are two important problems in the unilateral use of the thiol-ene reaction. First, the polymer dispersion reacts slowly even in the absence of initiating conditions during synthesis and storage.<sup>12</sup> Second, there is competition between the chain growth of acrylates and the free radical-mediated thiol-ene reaction under photoinitiator conditions. Cramer and Bowman<sup>13</sup> have shown that the rate constant of acrylate propagation is 1.5 times higher than that of extracting hydrogen from mercaptan, which leads to the existence of some unreacted mercaptan groups in the polymer network, which not only produce special odors but also lead to the degradation of material properties.<sup>14</sup> For these reasons, for the application of high-performance coatings, the improvement of chemical properties is necessary.

Therefore, in this study, thiol-isocyanate and thiol-ene click reactions were combined. In the first phase of this study, an initial homogeneous polymer network was synthesized by a thiol-isocyanate click reaction under the catalysis of organotin.<sup>15</sup> In this way, thiols are introduced into the main chain to form long polymer chains containing sulfhydryl groups with no odor. The thiocarbamate bond is similar to carbamate, which can form hydrogen bonds with carbonyl groups and has good mechanical strength.<sup>16,17</sup> In the second stage, the unsaturated carbon double bond-rich PETTA was introduced, and the remaining sulfhydryl groups were completely reacted by a thiol-ene click reaction. This does not affect the chain growth rate of the later acrylate, while generating thioether bonds with antioxidant resistance to polymerization, which can increase the light curing speed and conversion rate, as a way to reduce curing time and save energy.<sup>9</sup> Finally, under ultraviolet light, the remaining C=C groups are cured quickly to form an interpenetrating network polymer (IPN), which makes the material have good toughness and high hardness at the same time.

## Experimental

### Materials

Isophorone diisocyanate (IPDI) (99% purity) was obtained from Macklin Biochemical Co., Ltd. Polycarbonate diol (PCDL) (number-average molecular weight  $M_n$  is 1000, hydroxyl value is  $110 \pm 10$  KOH mg  $\text{g}^{-1}$ ) and

bisphenol-A diglycidyl ether (E-51) were acquired from Jining Huakai Resin Co., Ltd. (Shangdong, China). All polyols were dehydrated in vacuum at 120°C for 2 h before use. 1,4-Butanediol (BDO), stannous octanoate (T-9), dibutyltin dilaurate (T-12), triethylamine (TEA), and acetone were obtained from Sinopharm Chemical Reagent Co., Ltd. (China). Trimethylolpropane tris(3-mercaptopropionate) (TMPMP) (85% purity), photoinitiator 2959 (98% purity), pentaerythritol triacrylate (PETA) (95% purity, containing stabilizer MEHQ), and pentaerythritol tetraacrylate (PETTA) (95% purity, containing stabilizer MEHQ) were acquired from Meryer Chemical Technology Co., Ltd. (China). 2,2-Bis(hydroxymethyl)propionic acid (DMPA) (98% purity) was purchased from Wendong Chemical Co., Ltd. (China). 4-Methoxyphenol (MEHQ) (98% purity) was supplied by Bide Pharmatech Co., Ltd. (China).

### Synthesis of WPTU emulsion

The feed ratio of the WPTU prepolymer is listed in Table 1. First, the pretreated quantitative PCDL and IPDI were added to a four-necked flask with a reflux condenser, electric stirrer and thermometer. The prepolymerization reaction was carried out at 70°C for approximately 1 h. Second, after the temperature was cooled to approximately 50°C, catalyst T-9 and chain extenders DMPA, BDO and E-51 were added to extend the chain. The prepolymer of end-NCO was obtained by reacting for 4 h under these conditions. Third, different mass fractions of TMPMP and catalyst T-12 were slowly added to complete the end-capping reaction. Acetone was used to adjust the viscosity and heat dissipation during the reaction. TEA was added to the flask and stirred for 20–30 min to neutralize the carboxyl group. After the action, the mixture was emulsified by adding deionized water for 45 min of stirring at 1000  $\text{r min}^{-1}$  to obtain a waterborne thiopolyurethane emulsion. Finally, with the removal of acetone by a rotary evaporator, the emulsion was obtained with a solid content of 35%.

### Synthesis of WPTUA dispersion

The preparation procedure is outlined in Fig. 1. The synthesis steps of WPTUA are the same as those of WPTU. Before emulsification, a minor amount of TEA and PETTA were added and stirred for 30 min. Afterward, the mixture was emulsified by adding deionized water for 45 min with stirring at 1000  $\text{r min}^{-1}$  to obtain a UV-curable waterborne poly(thiourthane-urethane) acrylate dispersion.

### Synthesis of WPUA dispersion

Waterborne polyurethane acrylate (WPUA) is the blank control group of WPTUA. In the process of WPUA synthesis, TMPMP was not used for end-

**Table 1: The mass ratio of WPTU and WPTUA**

Sample designation	Composition of prepolymer (mass ratio)							
	IPDI	PCDL	BDO	E-51	DMPA	TMPMP	PETTA	TEA
WPTU-1	1	1.61	0.07	0.14	0.15	0.29	–	0.07
WPTU-2	1	1.61	0.07	0.14	0.15	0.44	–	0.07
WPTU-3	1	1.61	0.07	0.14	0.15	0.58	–	0.07
WPTU-4	1	1.61	0.07	0.14	0.15	0.73	–	0.07
WPTUA-1	1	1.61	0.07	0.14	0.15	0.58	0.66	0.07
WPTUA-2	1	1.61	0.07	0.14	0.15	0.58	0.86	0.07
WPTUA-3	1	1.61	0.07	0.14	0.15	0.58	1.13	0.07
WPTUA-4	1	1.61	0.07	0.14	0.15	0.58	1.39	0.07
WPTUA-5	1	1.61	0.07	0.14	0.15	0.58	1.68	0.07

The number is the ratio of the mass of each component to the mass of IPDI.

capping, but PETA with the same structure without sulfhydryl groups was used for end-capping. The subsequent synthesis steps were the same as those for WPTUA.

#### **Preparation of UV curing film and UV curing coating**

Photoinitiator 2959 (3 wt%) was added to the dispersion and mixed well. Then, it was cast on a poly(tetrafluoroethylene) sheet and dried at 45°C for 24 h. To obtain the UV-WPTU film, the poly sheet was exposed directly under the UV lamp. The film was cured in a UV curing light box, in which the wavelength of the UV lamp was 365 nm and the light intensity was 756 mJ cm<sup>-2</sup>. After curing, the film was peeled off for further testing.

Photoinitiator 2959 (3 wt%) was added to the dispersion and mixed well. Then, the mixture was coated on the PET substrate with a 50 μm filament stick. Finally, it was dried and exposed directly under a UV lamp to obtain WPTUA-covered PET material.

#### **Characterization**

##### *Performance of WPTU and WPTUA*

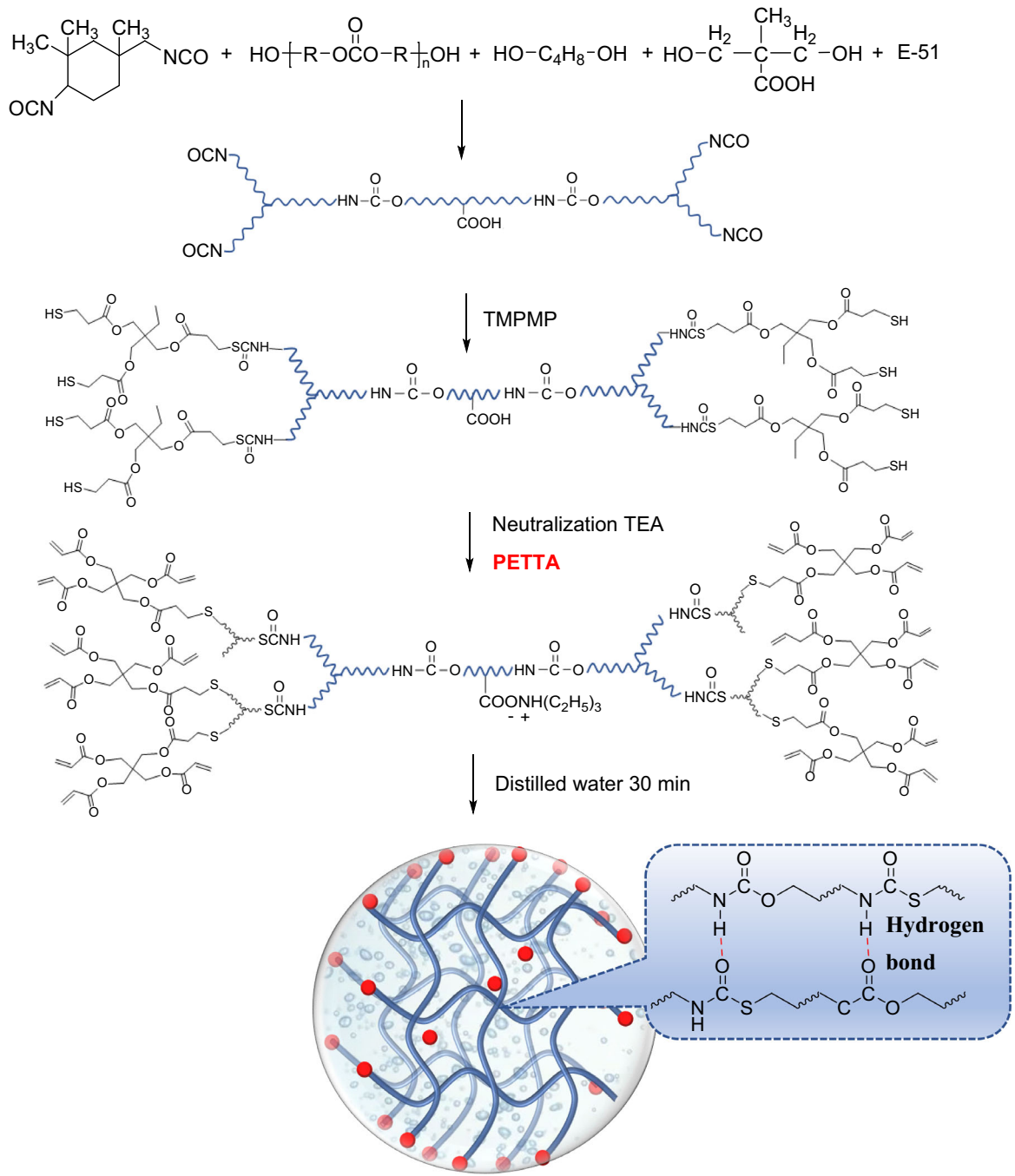
The FTIR spectra were obtained using a PerkinElmer Spectroscopy II. The functional groups were further analyzed with a Raman spectrometer produced by inVia-Reflex. Raman spectroscopy ranged from 100 to 3200 cm<sup>-1</sup> with an excitation source of 532 nm. The average particle size and its distribution in the dispersions were tested at room temperature by using a ZS-90 particle size analyzer. The dispersion stability was measured by using a TGL-16G high-speed centrifuge (China) at 3000 rpm for 15 min. If no stratification occurred after centrifugation, the dispersions could be assigned a shelf life of six months.

##### *Cured film properties*

Regarding the standard ASTM D882, the stress and strain of the film were measured by a universal material testing machine at a speed of 50 mm min<sup>-1</sup>. The Shore hardness was evaluated with a Shore durometer according to the standard ASTM D2240. Pencil hardness was measured with a pencil test according to standard ASTM D3363-05. Toughness was measured with a paint film flexibility tester in accordance with standard GB/T 1731-2020. Adhesion was measured by a tape test according to standard ASTM D3359, with adhesion grades from level 0 to level 5. Thermogravimetric analysis (TGA) was performed on a PerkinElmer TGA-7 with a heating rate of 10°C min<sup>-1</sup> under a nitrogen atmosphere, and the temperature range was 50–800°C. The water absorption ratio ( $A$ ) was calculated according to the following equation:  $A = (m_2 - m_1)/m_1 \times 100\%$ . The initial film was weighed and recorded as  $m_1$  and then soaked in deionized water at room temperature for 24 h, followed by wiping off the water on the surface of the film to determine the weight ( $m_2$ ). The gelation rate was calculated by the following equation:  $\text{Gelationrate}(\%) = m_0/m_1 \times 100\%$ , and the polymer cured film of mass  $m_1$  was soaked in toluene for 48 h. After drying, the mass of solid residue  $m_0$  was weighed.

##### *Curing performance test*

FTIR spectroscopy was used to detect the curing reaction of the film. The UV curing kinetic behavior can be evaluated by monitoring the change in the intensity of the =C–H bending (808 cm<sup>-1</sup>) peak.<sup>18</sup> In the research, the conversion rate of the cured film depends on the amount of C=C groups in the resin. The characteristic peak of the carbonyl group at approximately 1730 cm<sup>-1</sup> can be used to eliminate the effect of thickness scattering.<sup>19</sup> Using Origin software, the area under the peak was calculated by



E-51 fragments after reaction:

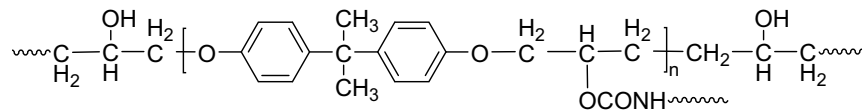


Fig. 1: The synthesis principle of a waterborne poly(thiourethane-urethane) acrylate dispersion

integration. Thus, the C=C group conversion ( $x$ ) after a preset irradiation time ( $t$ ) can be easily obtained from a particular absorbance region before ( $A_0$ ) and after UV irradiation ( $A_t$ ), as shown in the following equation:

$$X = \frac{(A_{808}/A_{1730})_0 - (A_{808}/A_{1730})_t}{(A_{808}/A_{1730})_0} \times 100(\%)$$

### Hydrogen bonding testing

FTIR spectroscopy was used to detect the degree of hydrogen bonding. In the Origin software, the three peaks of the IR spectrum curve ( $\sim 1740 \text{ cm}^{-1}$ ,  $\sim 1719 \text{ cm}^{-1}$ ,  $\sim 1696 \text{ cm}^{-1}$ ) were fitted by the Gauss function. Finally, the fitting data peak area percentage of

different C=O peaks was obtained, which corresponded to the corresponding bond concentration.

## Results and discussion

### Characterization of the WPTU and WPTUA

In Fig. 2a, there is a bending vibration absorption peak of =C-H at  $808 \text{ cm}^{-1}$ ,<sup>20</sup> the characteristic peak of carbamate at  $3345 \text{ cm}^{-1}$ , the absorption peak of C=O in -NHCOO- at  $1736 \text{ cm}^{-1}$ , and the stretching vibration peak of C-O-C in -NHCOO- at  $1242 \text{ cm}^{-1}$ .<sup>21</sup>

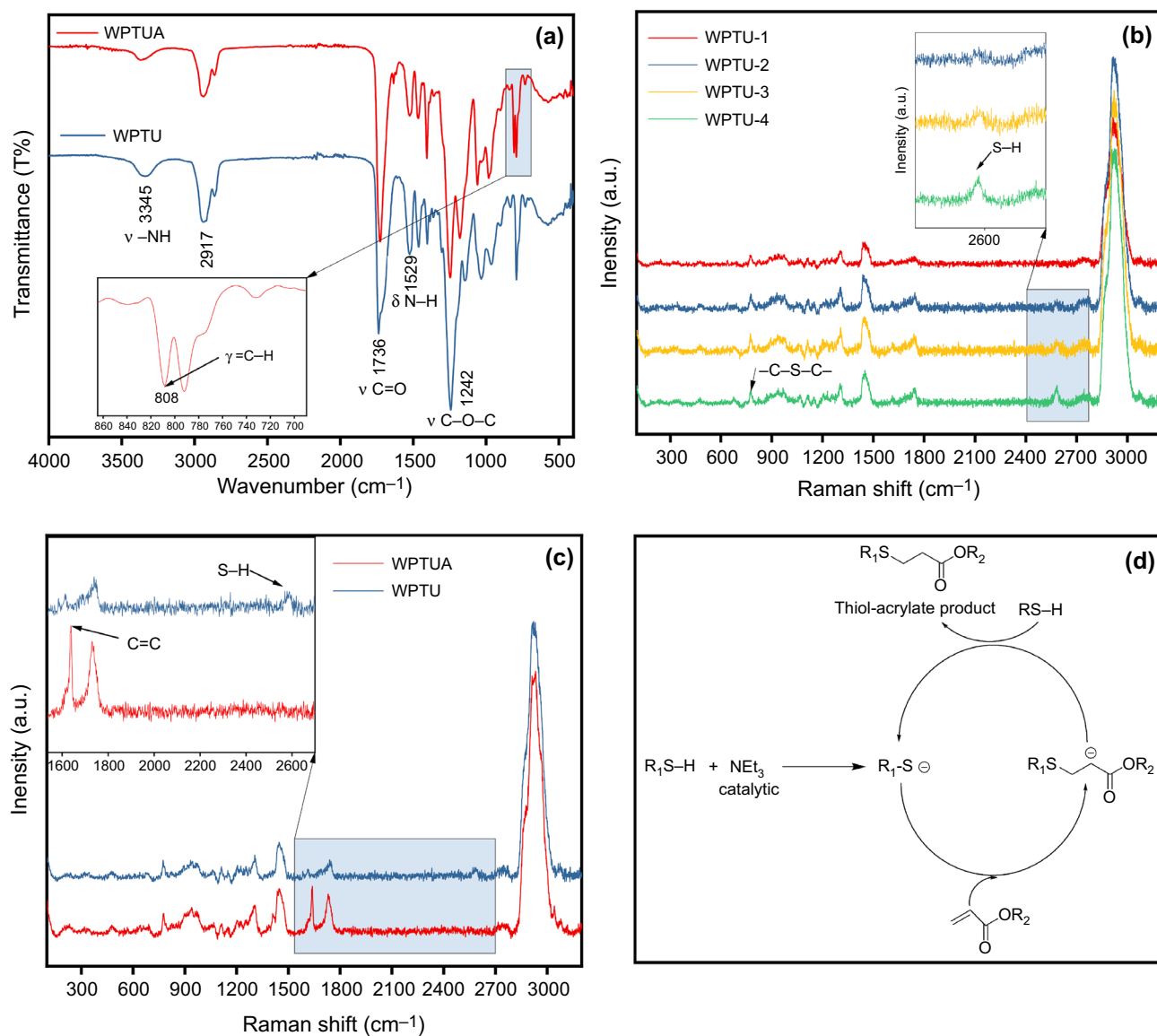


Fig. 2: (a) IR spectra of WPTU and WPTUA; (b) Raman spectra of WPTU under different reaction conditions (WPTU-1: TMPMP content 8 wt%, WPTU-2: TMPMP content 12 wt%, WPTU-3: TMPMP content 16 wt%, WPTU-4: TMPMP content 20 wt%); (c) Raman spectra of WPTU and WPTUA; (d) Mechanistic diagram of the thiol-acrylate Michael addition reaction

**Table 2: Mechanical properties of WPTU films**

Sample designation	Strain (%)	Stress (MPa)	Young's modulus
WPTU-1	361.4	36.01	390.5
WPTU-2	370.1	35.59	346.5
WPTU-3	467.4	37.62	383.2
WPTU-4	572.6	17.47	134.5

The structures of C=C, C–C and C–S in polymers have strong signal bands in Raman spectra, so the Raman spectrometer and FTIR spectra are combined to determine functional groups. Figure 2b shows the Raman spectrum of waterborne thiopolyurethane under different reaction conditions. The theoretical molar ratio of –SH/NCO of WPTU-1 is approximately 1, the signal peak of S–H is not seen at  $2580\text{ cm}^{-1}$ , and the signal peak of C–S–C is observed at  $740\text{ cm}^{-1}$ , indicating that there is a click chemical reaction between TMPMP and isocyanate, and there are no sulfhydryl groups in the system, which further indicates that the reaction is thorough.<sup>22</sup> When the TMPMP content is more than 8 wt%, the S–H stretching vibration peak appears at  $2580\text{ cm}^{-1}$  in Fig. 2b,<sup>23,24</sup> indicating the presence of sulfhydryl groups in the system, which can participate in the next step of the reaction. The signal peaks of WPTU-3 and WPTU-4 gradually became more intense with increasing TMPMP dosage, indicating an increase in sulfhydryl groups. In addition,  $2930\text{ cm}^{-1}$  is the C–H stretching vibration that produces the Fermi resonance effect.<sup>25</sup> In summary, waterborne thiopolyurethane emulsions with sulfhydryl group capping were successfully synthesized.

Figure 2c shows the Raman spectra of waterborne thiopolyurethane and waterborne poly(thiourethane-urethane) acrylate. When PETTA was introduced, the S–H peak of WPTU at  $2588\text{ cm}^{-1}$  disappeared in Fig. 2c, and the characteristic peak of the C=C group appeared at  $1638\text{ cm}^{-1}$  for WPTUA.<sup>26</sup> This result suggests that the thiol-ene click reaction between the sulfhydryl and C=C groups occurred under the conditions of triethylamine and that there were remaining C=C groups in the system. The reaction mechanism is Michael's addition reaction, as shown in Fig. 2d. The sulfhydryl group removes protons under the action of triethylamine. As a strong nucleophile,  $\text{R}_1\text{S}^-$  attacks the electron-philic  $\beta$ -carbon in the C=C group to form a carbon anion intermediate, which grabs a proton from the sulfhydryl group to form an antihorse addition structure. As a result, waterborne poly(thiourethane-urethane) acrylate dispersions were prepared.<sup>27</sup>

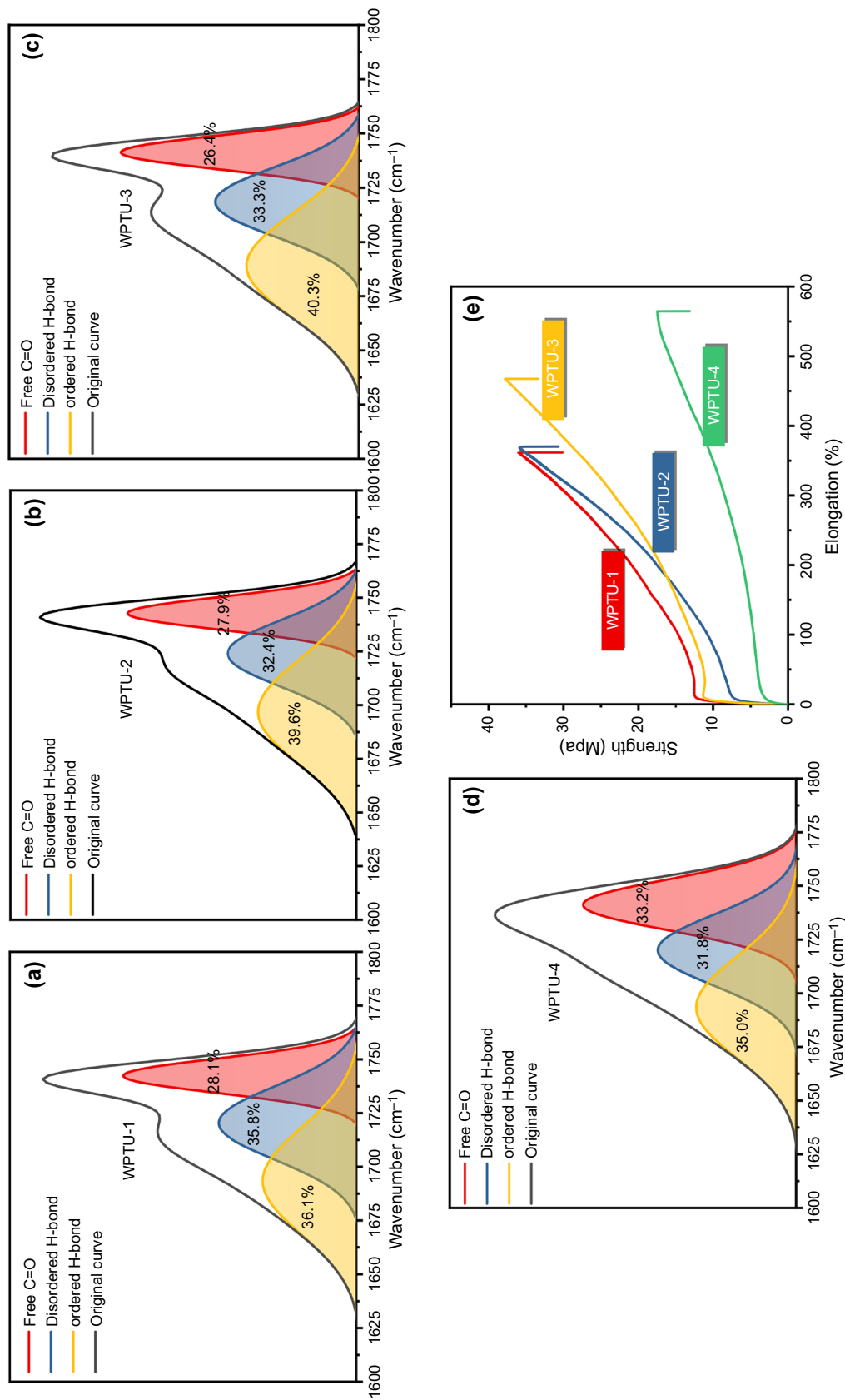
### Effect of TMPMP content on material properties

Table 2 shows that the strain increased with increasing concentrations of TMPMP, and the stress decreased, while Young's modulus also diminished.

As the content of TMPMP capping agent increases, the reactive active site with isocyanate in resin increases. The content of the hard segment increases since its good support can improve the tensile strength of the material. On the other hand, the growing network of isocyanate and sulfhydryl groups is a uniform, elastic and tough polymer. The carbamate bonds in the thiocarbamate network are very rigid and can form hydrogen bonds, so the polymer has a large stress.<sup>9</sup> Among them, the maximum stress of WPTU-3 is 37.62 MPa. When the content of TMPMP is excessive, there are too many residual monomers in the system, and the polymer network formed is relatively loose, so the stress decreases greatly. The stress of WPTU-4 decreased to 17.47 MPa. At the same time, the flexible and easily rotatable C–S–C content increases, and the molecular chain easily displaces and rearranges under the action of external forces, showing ductile behavior, so the strain increases continuously. The maximum strain of WPTU-4 is 572.6%. Young's modulus represents the physical quantity of the elasticity of the material itself and reflects the tensile resistance of the material. Because the C–S–C in the molecular chain can be shifted and rearranged, Young's modulus decreases gradually.

Hydrogen bonding allows the formation of a physically crosslinked network within polyurethane, resulting in a high density of cohesive energy, which has a significant influence on the mechanical properties of the material. Thus, we further investigated the relationship between the content of TMPMP and hydrogen bonding, and we tested FTIR and C=O spectra (from  $1600$  to  $1800\text{ cm}^{-1}$ ), as depicted in Fig. 3. Their degree of hydrogen bonding can be calculated.<sup>28</sup> In this region, three absorbance peaks have been observed: the absorbance at  $1740\text{ cm}^{-1}$  can be attributed to the unbonded carbonyls of the urethane and polycarbonate soft segments. The absorbance at  $1719\text{ cm}^{-1}$  is assigned to hydrogen-bonded urethane carbonyls in polycarbonate soft segments overlapped with loosely bonded urethane carbonyls, and the band at  $1696\text{ cm}^{-1}$  is assigned to hydrogen-bonded urethane carbonyls.<sup>29–31</sup> The diagram is represented by free C=O bonds, disordered H-bonds and ordered H-bonds.

Figure 3 shows that with increasing TMPMP content, the red area gradually decreases, indicating that the free carbonyl group gradually decreases. The yellow area gradually becomes larger and gradually turns into disordered and ordered H-bonds, suggesting that the number of H-bonds gradually increases and that there is extensive interaction between the carbonyl group and N–H in polyurethane, i.e., H-bonds are formed. The hydrogen bonding content of WPTU-3 reaches 73.6%, as seen in Fig. 3c, where the ordered hydrogen bonding reaches 40.3%, indicating that the hydrogen bonding force of WPTU-3 is the highest. As the TMPMP content continued to increase, the number of WPTU-4 ordered hydrogen bonds decreased significantly because when there were excessive capping agents in the system, the relative concentration of



**Fig. 3:** (a), (b), (c), (d) FTIR absorption spectra of the C=O groups of WPTU-1, WPTU-2, WPTU-3, and WPTU-4, respectively, in the stretching region. The 1740  $\text{cm}^{-1}$  (red-filled region), 1719  $\text{cm}^{-1}$  (blue-filled region), and 1696  $\text{cm}^{-1}$  (yellow-filled region) bands represent free carbonyl, disordered and ordered H-bonds, respectively. (e) Mechanical properties of waterborne thiopolyurethane (Color figure online)

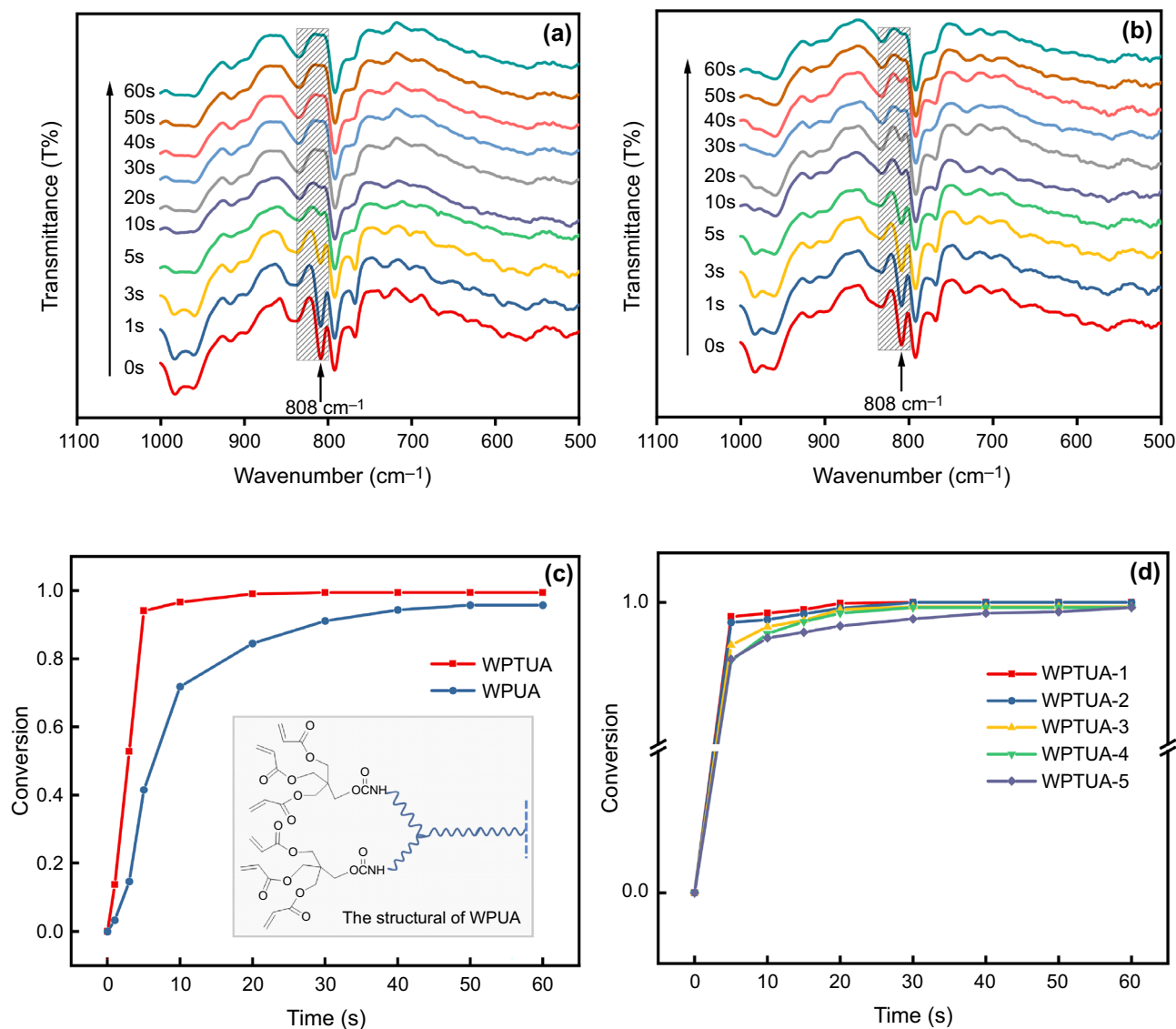


**Fig. 4:** (a) FTIR spectra of WPTUA and (b) WPUA; (c) The relationship between C=C conversion and light time for WPTUA and WPUA; (d) Relationship between the conversion rate of C=C groups with different contents and light time

urethane groups in the polymer decreased, thus reducing the hydrogen bond and intermolecular force in the polymer.

### Study of the photocuring process

The series of WPTUA-containing thioether bonds were synthesized by introducing different dose ratios of PETTA into the system. A blank group was set up to compare the effect of thioether bonds on the cured system. The FTIR spectrum was used to monitor the reduction of the bending peak of =C–H (808 cm<sup>-1</sup>). The FTIR spectra and conversions of C=C groups versus irradiation time of WPTUA and WPUA are shown in Fig. 4.

As shown in Fig. 4a, most of the C=C groups of WPTUA were cured at 5 s, and the C=C groups were

cured completely at 20 s. In Fig. 4b, the curing rate is relatively low for the blank control without thioether bonds in the case of containing the same amount of C=C groups. The C=C group conversion rate was still only 95.7% when exposed to ultraviolet light for 60 s. Further comparison of their conversion rates versus irradiation time is shown in Fig. 4c. The C=C group conversion rate of WPTUA is significantly higher than that of WPUA, indicating that the introduction of the thioether bond has a greater influence on the system.

In Fig. 5, the mechanism is that the initial radical or macromolecular radical can quickly react with oxygen molecules to generate a peroxy radical without initiation activity, and then the peroxy radical can seize the hydrogen atom on the α-C of the thioether bond to generate a new radical that continues to initiate the polymerization reaction of the unsaturated C=C group,



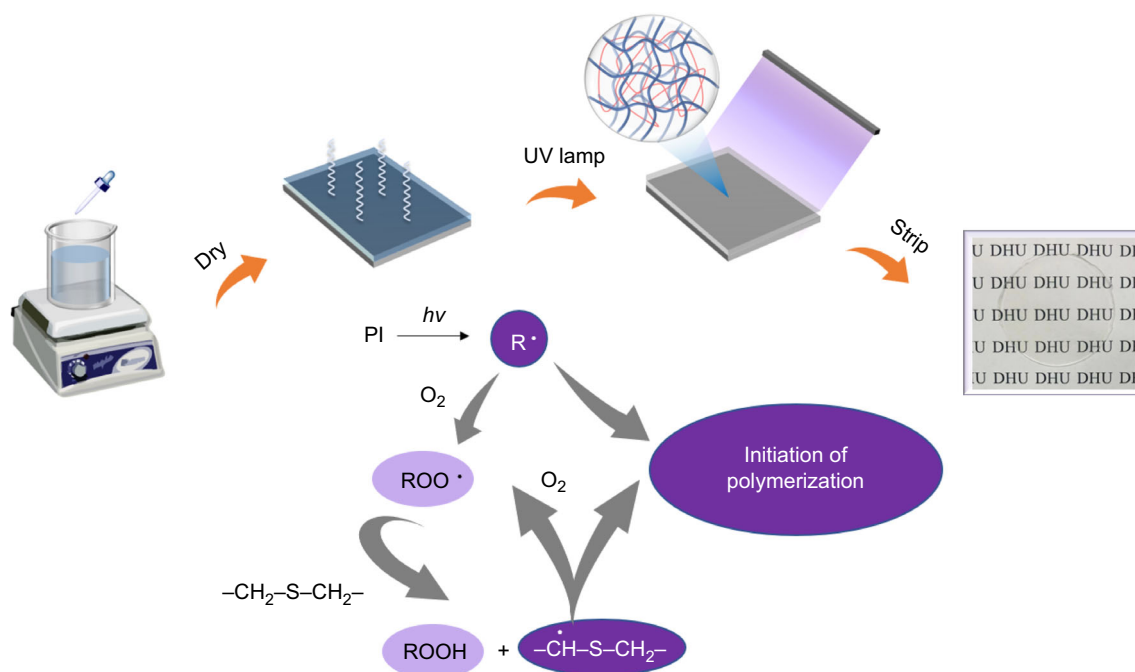


Fig. 5: The mechanism of thioether to overcome the oxygen blocking effect and film preparation process

Table 3: Properties of UV-WPTU films

Sample designation	Hardness		Flexibility (mm)	Adhesion	Water absorption rate (%)	Gelation rate (%)
	Pencil hardness	Shore hardness				
WPTUA-1	H	50 ± 0.3	1	0	6.61	89.62
WPTUA-2	2H	52 ± 0.6	1	0	4.65	90.43
WPTUA-3	3H	59 ± 0.7	1	0	1.79	91.49
WPTUA-4	3H	62 ± 0.4	1	0	2.14	92.24
WPTUA-5	4H	70 ± 0.5	2	1	3.52	96.50

thus effectively overcoming the oxygen-blocking polymerization.<sup>32</sup> Figure 4d shows that the conversion rates of WPTUA-1, WPTUA-2 and WPTUA-3 remained at a high level, and 100% curing could be achieved with increasing C=C group content in the system. However, when the content of PETTA is excessive, due to the decrease in the relative content of thioether bonds and the weak antipolymerization effect, the conversion of the C=C group of WPTUA-5 decreases slightly, but the conversion rate of the C=C group can still be maintained at 99.4% by prolonging the curing time. This shows that WPTUA can achieve a high conversion rate and cure in a short time.

### Coating performance

Figure 5 shows the preparation process of the film. It is shown that the film is extremely transparent. Table 3

shows the pencil hardness, Shore hardness, toughness, adhesion, water absorption and gelation rate of UV-WPTUA films. The pencil hardness of UV-WPTUA films ranges from H-4H, with Shore D values between 50 and 70, and the higher the degree of crosslinking as the PETTA content increases, the higher the film hardness.

When the coating is coated on a PET substrate, the best adhesion can reach grade 0 because WPTU contains a large number of polar carbonyl, urea and ester groups, which can be closely bonded to the ester group and terminal hydroxyl group on the PET group by chemical bonding, and the excellent adhesion of thioether bonds also plays a certain role, so the UV cured film shows excellent adhesion.<sup>32</sup> The adhesion of WPTUA-5 is slightly reduced because the addition of a crosslinking agent destroys the regularity of the molecular chains. It decreases the crystallinity of the polymer and affects the movement of molecular chains,

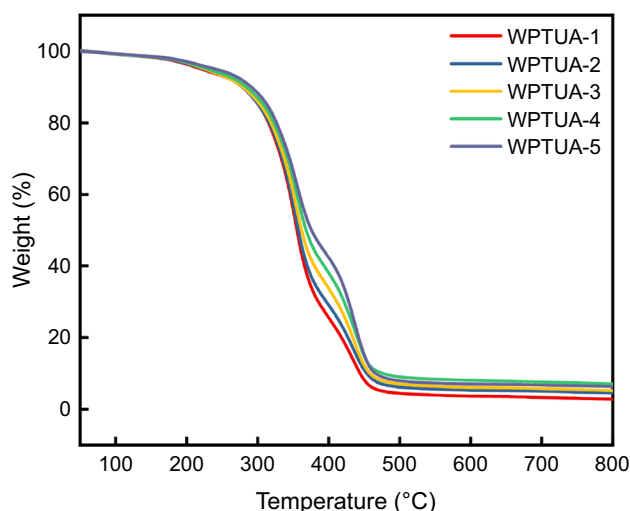


Fig. 6: TGA curve of UV-curable film

resulting in a decrease in the density of hydrogen bonds between the polyurethane molecules and the substrate.<sup>33</sup> The best flexibility can also be seen in Table 3 to reach level 1, which is mainly because the thioether bond can give the material good flexibility.

Waterborne polyurethane has the ability to disperse in water because of its hydrophilic groups. Correspondingly, the affinity for water molecules increases significantly after film formation, resulting in poor water resistance of the cured film.<sup>34</sup> Table 3 shows that the water absorption rate shows a trend of increasing first and then declining. As the PETTA content increases, the degree of crosslinking increases. The high crosslink density can prevent water molecules from penetrating inside the film and prevent hydrophilic groups from moving to the surface, so the water absorption rate gradually decreases. The water absorption rate of WPTUA-3 is the lowest at 1.79%.<sup>35</sup> The water absorption rates of WPTUA-4 and WPTUA-5 are slightly increased because the crosslinking degree between WPTUA-4 and WPTUA-5 further increases. Second, the mutual integration of latex particles becomes poor, resulting in difficult intermolecular sliding. Third, the flexibility of the film decreases, making it easy for water molecules to penetrate from outside to inside at this time, resulting in an increase in the water absorption rate. On the other hand, the water resistance of the ester bond is worse than that of the thioether bond, and the concentration of thioether bonds in WPTUA-4 and WPTUA-5 is relatively low, so the water resistance is poor.<sup>36</sup>

The crosslinked entangled fraction of the cured sample is insoluble in the solvent. Therefore, the gelation rate and percentage of insoluble cured samples can represent the degree of crosslinking. In Table 3, the gelation rate of the cured films ranged from 91.51% to 95.5%, showing a high degree of crosslinking of the cured samples. Due to the addition

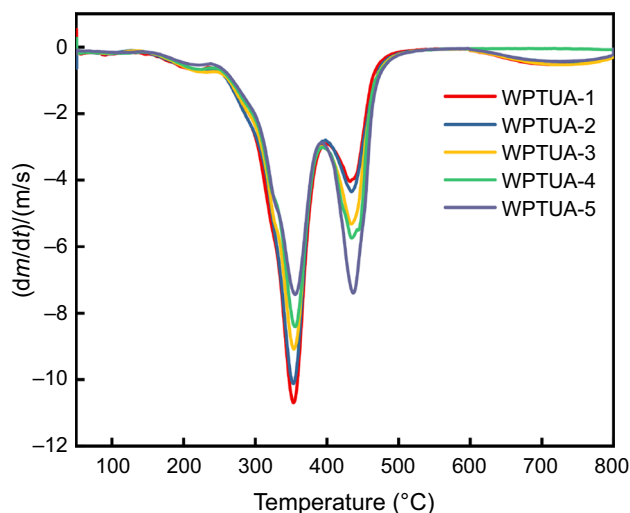


Fig. 7: DTG curve of UV-curable film

of sulfhydryl-Michael, PETTA is partially embedded in the cured film, and the C=C group at the chain end reacts with the sulfhydryl group located on the main chain to form a network interpenetration structure. When the PETTA content increases, the structure of the polymer network becomes denser, so the gelation rate of WPTUA gradually increases.

### Thermal gravimetric analysis

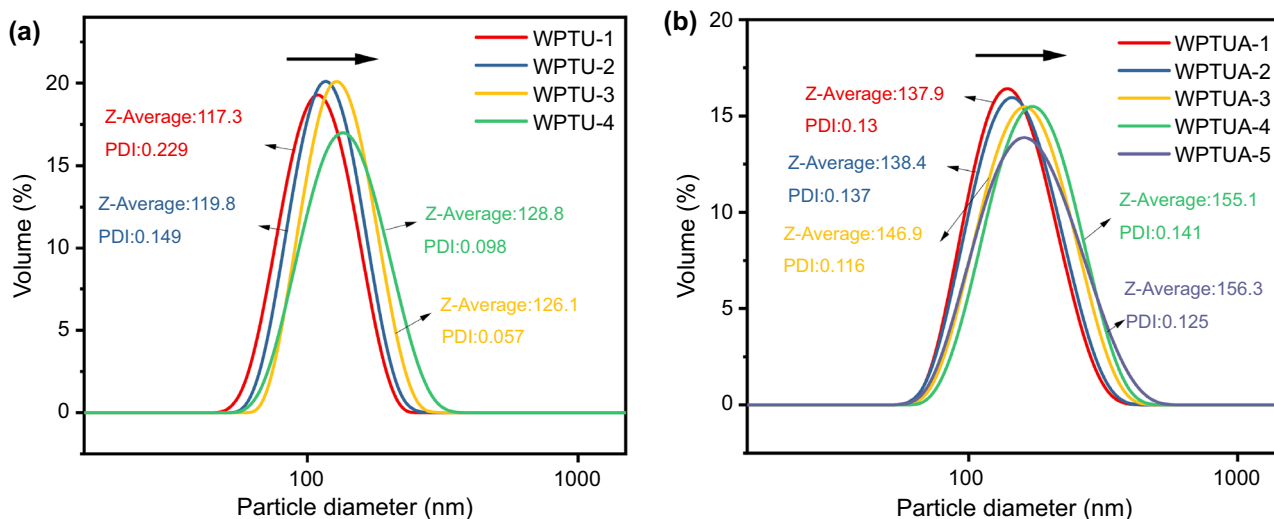
Thermogravimetric analysis (TGA) and thermal gravity difference (DTG) are the main methods for characterizing the thermal stability of materials. Figure 6 shows the TGA and DTG curves of the cured films, resulting in 10% and 50% loss mass and residual mass.

For WPTUA, the onset of decomposition temperature is influenced by two aspects. One is the influence of the crosslink density of the system. The influence of the soft and hard segment content is the other. As the PETTA content increases, the degree of crosslinking of the film increases, resulting in an increase in  $T_{10\%}$  of the cured film from 278.1 to 290.6°C and  $T_{50\%}$  from 355.3 to 375.8°C. The abundance of C=C groups in the FTIR spectra is the main cause of this. The high density of the crosslinked network formed and the high cohesion energy require a higher temperature to destroy the structure of the molecular chain. Therefore, the resin requires a higher temperature for thermal decomposition to occur. The thermal stability values ( $T_{10\%}$  and  $T_{50\%}$ ) of WPTUA-1, WPTUA-2 and WPTUA-3 are very similar, probably because the relative concentrations of thioether bonds are relatively close to each other, so they all exhibit good thermal stability under an inert atmosphere.

Two weight loss peaks in the DTG curves of WPTUA cured films can be seen in Fig. 7, where the first weight loss peak (340–360°C) is the decomposition of carbamate and urea groups in WPUA, and the

**Table 4: TGA and DTG data of cured WPTUA**

Sample designation	Decomposition temperature		Peaks of deriv. weight (°C)		
	$T_{10\%}$	$T_{50\%}$	First	Second	Residues (wt%)
WPTUA-1	278.1	355.3	352.9	438.4	2.71
WPTUA-2	278.1	357.3	352.8	435.3	4.48
WPTUA-3	278.9	361.8	353.6	435.4	5.14
WPTUA-4	283.7	368.3	353.1	437.1	5.98
WPTUA-5	290.6	375.8	357.8	439.8	6.26

**Fig. 8: (a) Particle size distribution of aqueous thiopolyurethane; (b) particle size distribution of waterborne thiopolyurethane acrylate**

second weight loss peak (430–440°C) is related to the decomposition of soft segments in WPUA.<sup>37</sup>

The DTG curve shows that the decomposition rate of the hard segment is significantly higher than the decomposition rate of the soft segment, which is unfavorable to the thermal stability of the cured film. In Table 4, with increasing PETTA content, the decomposition rate of the hard segment gradually decreases. This is because the formation of a three-dimensional network structure causes the hard and soft segments of the polymer to intertwine with each other, and the energy barrier of molecular chain movement increases, resulting in a gradual decrease in the decomposition rate of the hard segment and a gradual increase in the residual mass, indicating that the higher the content of C=C groups is, the better the density and thermal stability of the film.

#### **Storage stability of WPTU and WPTUA dispersions**

The average particle size of waterborne polyurethane emulsions and their distribution are used to evaluate

the polymer emulsion stability. Products with good emulsion stability are beneficial for long-term preservation. As seen in Fig. 8a, the average particle size was between 117.3–126.1 nm. The average particle size gradually increased as the amount of TMPMP increased because the concentration of ionic groups per unit chain length of the prepolymer decreased, and the average particle size gradually increased as the ionic content decreased in the stabilization mechanism of the ionomer emulsion.<sup>38</sup> The distribution index of the emulsion was between 0.057 and 0.229, which was normally distributed. In summary, the effect of TMPMP concentration on the emulsion particle size is not significant.

From Fig. 8b, it can be seen that with the introduction of PETTA, the dispersion average particle size is between 137.9–156.3 nm with a normal distribution. This shows that PETTA can be wrapped in dispersed particles by the chain segments. The ionic groups are mainly situated on the particle surface. At the interface between the particles and water, the ionic groups dissociate to form electrical bilayers, so a stable dispersion is obtained. As the amount of PETTA increases, the hydrophobicity becomes stronger, and the stabiliz-

ing ability of the chain segments dispersed on the ionic surface acting as dispersions decreases, which is the reason why the average particle size increases.<sup>21</sup> In general, the dispersion with a particle size less than 200 nm has better stability, and the distribution index of the dispersion is between 0.125–0.141, which indicates that the dispersion still has good monodispersity. After the centrifugal stability test, there was no delamination, indicating that WPTUA dispersions can also be left at room temperature for more than 6 months.

## Conclusions

In this study, UV-curable waterborne poly(thiourethane-urethane) acrylate coatings produced by thiol-click chemistry were green and odorless. The contents of TMPMP and PETTA were also explored. When the content of TMPMP reaches 16 wt% and the content of PETTA reaches 28 wt%, the interpenetrating network structure is the most perfect, and the thioether bond introduced into the polymer main chain has an effective antioxygen inhibition effect to reduce the curing time and energy consumption. The obtained cured film has excellent mechanical properties. The adhesion and toughness of the film are the best, the pencil hardness reaches 3H, the Shore hardness D value reaches 62, the overall rigidity is strong, and the mechanical strength is good, so it is suitable for the protective film on the surface of the fragile substrate. Meanwhile, the film has efficient light-curing behavior and excellent water and heat resistance, increasing the scope of its application.

**Acknowledgments** The authors would like to thank Key Laboratory of Science & Technology of Eco-Textile of Ministry of Education for their kindness of providing the Laboratory facilities. This research did not receive any specific grant from funding agencies in the public, commercial, or not-for-profit sectors.

**Conflict of interest** None.

## References

- Jiang, B, Shi, X, Zhang, T, Huang, Y, “Recent Advances in UV/Thermal Curing Silicone Polymers.” *Chem. Eng. J.*, **435** 134843–134858 (2022)
- Wang, X, Zhang, J, Liu, J, Luo, J, “Phytic Acid-Based Adhesion Promoter for UV-Curable Coating: High Performance, Low Cost, and Eco-friendliness.” *Prog. Org. Coat.*, **167** 106834–106844 (2022)
- Lim, KS, Galarraga, JH, Cui, X, Lindberg, GCJ, Burdick, JA, Woodfield, TBF, “Fundamentals and Applications of Photo-Cross-Linking in Bioprinting.” *Chem. Rev.*, **120** (19) 10662–10694 (2020)
- Konuray, O, Fernández-Francos, X, Ramis, X, Serra, À, “New Allyl-Functional Catalytic Comonomers for Sequential Thiol-Michael and Radical Thiol-ene Reactions.” *Polymer*, **138** 369–377 (2018)
- Hoyle, CE, Lowe, AB, Bowman, CN, “Thiol-click Chemistry: A Multifaceted Toolbox for Small Molecule and Polymer Synthesis.” *Chem. Soc. Rev.*, **39** (4) 1355–1387 (2010)
- Lowe, AB, Hoyle, CE, Bowman, CN, “Thiol-ene Click Chemistry: A Powerful and Versatile Methodology for Materials Synthesis.” *J. Mater. Chem.*, **20** (23) 4745 (2010)
- Hensarling, RM, Rahane, SB, LeBlanc, AP, Sparks, BJ, White, EM, Locklin, J, Patton, DL, “Thiol-isocyanate ‘Click’ Reactions: Rapid Development of Functional Polymeric Surfaces.” *Polym. Chem.*, **2** (1) 88–90 (2011)
- Ireni, NG, Narayan, R, Basak, P, Raju, KVS, “Poly(thiourethane-urethane)-urea as Anticorrosion Coatings with Impressive Optical Properties.” *Polymer*, **97** 370–379 (2016)
- Podgorski, M, Nair, DP, Chatani, S, Berg, G, Bowman, CN, “Programmable Mechanically Assisted Geometric Deformations of Glassy Two-Stage Reactive Polymeric Materials.” *ACS Appl. Mater. Interfaces*, **6** (9) 6111–6119 (2014)
- Yang, Z, Wicks, DA, Yuan, J, Pu, H, Liu, Y, “Newly UV-Curable Polyurethane Coatings Prepared by Multifunctional Thiol- and Ene-terminated Polyurethane Aqueous Dispersions: Photopolymerization Properties.” *Polymer*, **51** (7) 1572–1577 (2010)
- Chen, G, Guan, X, Xu, R, Tian, J, He, M, Shen, W, Yang, J, “Synthesis and Characterization of UV-Curable Castor Oil-Based Polyfunctional Polyurethane Acrylate via Photo-click Chemistry and Isocyanate Polyurethane Reaction.” *Prog. Org. Coat.*, **93** 11–16 (2016)
- Yang, Z, Wicks, DA, Hoyle, CE, Pu, H, Yuan, J, Wan, D, Liu, Y, “Newly UV-Curable Polyurethane Coatings Prepared by Multifunctional Thiol- and Ene-terminated Polyurethane Aqueous Dispersions Mixtures: Preparation and Characterization.” *Polymer*, **50** (7) 1717–1722 (2009)
- Cramer, NB, Bowman, CN, “Kinetics of Thiol-ene and Thiol-acrylate Photopolymerizations With Real-Time Fourier Transform Infrared.” *J. Polym. Sci. Part A: Polym. Chem.*, **39** (19) 3311–3319 (2001)
- Mishra, V, Desai, J, Patel, KI, “High-Performance Waterborne UV-Curable Polyurethane Dispersion Based on Thiol-acrylate/Thiol-epoxy Hybrid Networks.” *J. Coat. Technol. Res.*, **14** (5) 1069–1081 (2017)
- Jia, Y, Shi, B, Jin, J, Li, J, “High Refractive Index Polythiourethane Networks with High Mechanical Property via Thiol-isocyanate Click Reaction.” *Polymer*, **180** 121746 (2019)
- Li, Q, Zhou, H, Wicks, DA, Hoyle, CE, “Thiourethane-Based Thiol-ene High Tg Networks: Preparation, Thermal, Mechanical, and Physical Properties.” *J. Polym. Sci. Part A: Polym. Chem.*, **45** (22) 5103–5111 (2007)
- Fan, C, Wen, Z, Xu, Z, Xiao, Y, Wu, D, Yang, K, Wang, Y, “Adaptable Strategy to Fabricate Self-Healable and Reversible Poly(thiourethane-urethane) Elastomers via Reversible Thiol-Isocyanate Click Chemistry.” *Macromolecules*, **53** (11) 4284–4293 (2020)
- Xu, J, Jiang, Y, Zhang, T, Dai, Y, Yang, D, Qiu, F, Yu, Z, Yang, P, “Synthesis of UV-Curing Waterborne Polyurethane-Acrylate Coating and Its Photopolymerization Kinetics Using FT-IR and Photo-DSC Methods.” *Prog. Org. Coat.*, **122** 10–18 (2018)
- Wu, J, Ma, G, Li, P, Ling, L, Wang, B, “Surface Modification of Nanosilica with Acrylsilane-Containing Tertiary Amine

- Structure and Their Effect on the Properties of UV-Curable Coating." *J. Coat. Technol. Res.*, **11** (3) 387–395 (2014)
20. Bai, CY, Zhang, XY, Dai, JB, Li, WH, "A New UV Curable Waterborne Polyurethane: Effect of CC Content on the Film Properties." *Prog. Org. Coat.*, **55** (3) 291–295 (2006)
  21. Yuan, C, Wang, M, Li, H, Wang, Z, "Preparation and Properties of UV-Curable Waterborne Polyurethane-Acrylate Emulsion." *J. Appl. Polym. Sci.*, **134** (34) 45208 (2017)
  22. Liu, Y, Lu, J, Ge, C, Liu, M, Wang, H, "Study on Synthesis of High Molecular Weight Linear Polyphenylene Sulfide with Soluble Polyfluorene Cation as Precursor." *China Plast. Ind.*, **47** (5) 153–157 (2019)
  23. Murphy, GM, Vance, JE, "Raman Spectra of Hydrogen and Deuterium Sulfides in the Gas, Liquid and Solid States." *J. Chem. Phys.*, **6** (8) 426–429 (1938)
  24. Jiang, L, Xin, Y, Chou, IM, Chen, Y, "Raman Spectroscopic Measurements of  $\nu_1$  Band of Hydrogen Sulfide Over a Wide Range of Temperature and Density in Fused-Silica Optical Cells." *J. Raman Spectrosc.*, **49** (2) 343–350 (2018)
  25. Yuan, Y, Wang, M, Qu, Y, Zhang, Z, Zhang, J, "Application of Raman Spectroscopy in the Characterization of Polymers." *Acta Polym. Sin.*, **52** (9) 1206–1220 (2021)
  26. Berhe, DT, Eskildsen, CE, Lametsch, R, Hviid, MS, van den Berg, F, Engelsen, SB, "Prediction of Total Fatty Acid Parameters and Individual Fatty Acids in Pork Backfat Using Raman Spectroscopy and Chemometrics: Understanding the Cage of Covariance Between Highly Correlated Fat Parameters." *Meat Sci.*, **111** 18–26 (2016)
  27. Nair, DP, Podgórski, M, Chatani, S, Gong, T, Xi, W, Fenoli, CR, Bowman, CN, "The Thiol-Michael Addition Click Reaction: A Powerful and Widely Used Tool in Materials Chemistry." *Chem. Mater.*, **26** (1) 724–744 (2013)
  28. Chattopadhyay, DK, Raju, KVS, "Structural Engineering of Polyurethane Coatings for High Performance Applications." *Prog. Polym. Sci.*, **32** (3) 352–418 (2007)
  29. Hernandez, R, Weksler, J, Padsalgikar, A, Choi, T, Angelo, E, Lin, JS, Xu, L-C, Siedlecki, CA, Runt, J, "A Comparison of Phase Organization of Model Segmented Polyurethanes with Different Intersegment Compatibilities." *Macromolecules*, **41** (24) 9767–9776 (2008)
  30. Phua, SL, Yang, L, Toh, CL, Huang, S, Tsakadze, Z, Lau, SK, Mai, YW, Lu, X, "Reinforcement of Polyether Polyurethane with Dopamine-Modified Clay: The Role of Interfacial Hydrogen Bonding." *ACS Appl. Mater. Interfaces*, **4** (9) 4571–4578 (2012)
  31. Sami, S, Yildirim, E, Yurtsever, M, Yurtsever, E, Yilgor, E, Yilgor, I, Wilkes, GL, "Understanding the Influence of Hydrogen Bonding and Diisocyanate Symmetry on the Morphology and Properties of Segmented Polyurethanes and Polyureas: Computational and Experimental Study." *Polymer*, **55** (18) 4563–4576 (2014)
  32. Hoyle, CE, Lee, TY, Roper, T, "Thiol-enes: Chemistry of the Past with Promise for the Future." *J. Polym. Sci. Part A: Polym. Chem.*, **42** (21) 5301–5338 (2004)
  33. Shen, J, Zhang, H, Zhu, J, Ma, Y, He, H, Zhu, F, Jia, L, Zheng, Q, "Simple Preparation of a Waterborne Polyurethane Crosslinked Hydrogel Adhesive With Satisfactory Mechanical Properties and Adhesion Properties." *Front. Chem.*, **10** 855352 (2022)
  34. Honarkar, H, "Waterborne Polyurethanes: A Review." *J. Dispers. Sci. Technol.*, **39** (4) 507–516 (2017)
  35. Bai, CY, Zhang, XY, Dai, JB, Zhang, CY, "Water Resistance of the Membranes for UV Curable Waterborne Polyurethane Dispersions." *Prog. Org. Coat.*, **59** (4) 331–336 (2007)
  36. Xiao, Y, Bao, L, Fu, X, Wu, B, Kong, W, Zhou, C, Lei, J, "Effect of Phase Separation on Water Resistance of Green Waterborne Polyurethanes: Unexpected Stronger Impact Compared to Hydrophilic Segments." *Adv. Polym. Technol.*, **37** (6) 1618–1624 (2018)
  37. Cui, X, Liu, B, He, C, Tian, H, "Research on Thermal Degradation Mechanism and Thermal Stability of Aliphatic Polyether-Polyurethane Elastomer." *Chem. Ind. Eng. Prog.*, **35** (11) 3585–3589 (2016)
  38. Asif, A, Shi, W, Shen, X, Nie, K, "Physical and Thermal Properties of UV Curable Waterborne Polyurethane Dispersions Incorporating Hyperbranched Aliphatic Polyester of Varying Generation Number." *Polymer*, **46** (24) 11066–11078 (2005)

**Publisher's Note** Springer Nature remains neutral with regard to jurisdictional claims in published maps and institutional affiliations.

Springer Nature or its licensor (e.g. a society or other partner) holds exclusive rights to this article under a publishing agreement with the author(s) or other rightsholder(s); author self-archiving of the accepted manuscript version of this article is solely governed by the terms of such publishing agreement and applicable law.